

RESEARCH

Open Access



Diagnostic efficiency on ultrasound shear wave elastography in evaluation of steatosis severity for non-alcoholic fatty liver disease: a rat model

Yuhui Wu¹, Qianjiao Liu¹, Yan Wang¹, Fangyan Li¹, Lawrence Wing-Chi Chan³, Yong Wen¹, Fan Yang⁴, Yining Xiang⁵, Qinghong Duan¹, Peng Luo² and Pinggui Lei^{1,2,3*}

Abstract

Background The pathological feature of steatosis affects the elasticity values measured by shear wave elastography (SWE) is still controversial in non-alcoholic fatty liver disease (NAFLD). The aim of this study is to demonstrate the influence of steatosis on liver stiffness measured by SWE on a rat model with NAFLD and analyze feasibility of SWE for grading steatosis in absence of fibrosis.

Methods Sixty-six rats were fed with methionine choline deficient diet or standard diet to produce various stages of steatosis; 48 rats were available for final analysis. Rats underwent abdominal ultrasound SWE examination and pathological assessment. Liver histopathology was analyzed to assess the degree of steatosis, inflammation, ballooning, and fibrosis according to the non-alcoholic fatty liver disease activity score. The diagnostic performance of SWE for differentiating steatosis stages was estimated according to the receiver operating characteristic (ROC) curve. Decision curve analysis (DCA) was conducted to determine clinical usefulness and the areas under DCA (AUDCAs) calculated.

Results In multivariate analysis, steatosis was an independent factor affecting the mean elastic modules ($B = 1.558$, $P < 0.001$), but not inflammation ($B = -0.031$, $P = 0.920$) and ballooning ($B = 0.216$, $P = 0.458$). After adjusting for inflammation and ballooning, the AUROC of the mean elasticity for identifying $S \geq S1$ was 0.956 (95%CI: 0.872–0.998) and the AUDCA, 0.621. The AUROC for distinguishing $S \geq S2$ and $S = S3$ was 0.987 (95%CI: 0.951–1.000) and 0.920 (95%CI: 0.816–0.986) and the AUDCA was 0.506 and 0.256, respectively.

Conclusions Steatosis is associated with liver stiffness and SWE may have the feasibility to be introduced as an assistive technology in grading steatosis for patients with NAFLD in absence of fibrosis.

Keywords Shear wave elastography, Non-alcoholic fatty liver disease, Hepatic steatosis, Methionine choline deficiency, Fat quantification

*Correspondence:

Pinggui Lei
pingguilei@foxmail.com

¹ Department of Radiology, the Affiliated Hospital of Guizhou Medical University, No. 28 Guiyi Street, Yunyan District, Guiyang 550004, Guizhou, China

² School of Public Health, Guizhou Medical University, Guiyang, Guizhou, China

³ Department of Health Technology and Informatics, The Hong Kong Polytechnic University, Hong Kong, SAR, China

⁴ School of Biology & Engineering, Guizhou Medical University, Guiyang, Guizhou, China

⁵ Department of Pathology, The Affiliated Hospital of Guizhou Medical University, Guiyang, Guizhou, China



© The Author(s) 2023. **Open Access** This article is licensed under a Creative Commons Attribution 4.0 International License, which permits use, sharing, adaptation, distribution and reproduction in any medium or format, as long as you give appropriate credit to the original author(s) and the source, provide a link to the Creative Commons licence, and indicate if changes were made. The images or other third party material in this article are included in the article's Creative Commons licence, unless indicated otherwise in a credit line to the material. If material is not included in the article's Creative Commons licence and your intended use is not permitted by statutory regulation or exceeds the permitted use, you will need to obtain permission directly from the copyright holder. To view a copy of this licence, visit <http://creativecommons.org/licenses/by/4.0/>. The Creative Commons Public Domain Dedication waiver (<http://creativecommons.org/publicdomain/zero/1.0/>) applies to the data made available in this article, unless otherwise stated in a credit line to the data.

Background

Non-alcoholic fatty liver disease (NAFLD) is a chronic disease characterized by hepatic fat accumulation combined with underlying metabolic dysregulation, mainly encompassing hepatic steatosis, non-alcoholic steatohepatitis (NASH), non-alcoholic cirrhosis, and even hepatocellular carcinoma [1, 2]. It is rapidly becoming one of the most common liver diseases, with a 20–30% incidence in Western countries [3].

Liver biopsy (LB) is regarded as the gold standard for assessing disease severity [4, 5]. However, due to tissue invasion, sampling error, and the associated complications [6], imaging methods are increasingly being favored for the non-invasive evaluation of fatty liver. B-Mode Ultrasound (US) based on grayscale images is the most common method for evaluating fatty liver due to its low cost, safety, and availability. Hepatic steatosis is usually graded by various US features, including liver brightness, the hepatorenal ratio, and vessel blurring [7, 8]. However, the sensitivity of US B-mode imaging for detecting mild steatosis (fat content > 5%) is reportedly between 60.9% and 65% [9], and it does not allow quantitative evaluation. Although the controlled attenuation parameter (CAP) based on Fibroscan can accurately detect and quantify liver steatosis (> 10%), a meta-analysis showed that overlapping boundaries limit CAP's clinical value in distinguishing between mild and moderate steatosis [10, 11]. Liver ultrasound attenuation (LiSA) is a new technique similar to CAP, but it may not accurately reflect the actual performance of LiSA tested in LB-validated patients [12]. In contrast, Sound Speed Estimation could detect and grade hepatic steatosis with a sensitivity of 80% and specificity of 85.7% in a small pilot study, whereas further research in a larger sample of patients with NAFLD is needed [13].

Although CT is more effective in assessing fatty liver, it is less accurate for mild to moderate hepatic steatosis, and involves radiation exposure [14]. Magnetic resonance spectroscopy is a non-invasive method for the quantification of liver fat with high sensitivity and specificity; nevertheless, at present it is mainly used as a research tool [15].

Ultrasound elastography techniques, like transient elastography (TE), shear wave elastography (SWE), or acoustic radiation force impulse (ARFI), based on shear wave generation, aim to measure elasticity [16]. TE showed a great performance when identifying and staging fibrosis in NAFLD, but steatosis or inflammatory activity may influence the accuracy of liver stiffness measurements (LSMs) in predicting fibrosis [17–19]. A large-scale meta-analysis has shown that 2D-SWE is superior to TE in diagnosing significant fibrosis and cirrhosis [20]. However, whether steatosis affects the elasticity values

measured by SWE is still controversial [21]. Some studies found no correlation between steatosis and SWE measurements based on multivariate analysis [22, 23], whereas others have shown increasing liver viscoelasticity with the presence of steatosis [24].

Hence, we performed an experimental study in rats that had undergone SWE examinations, using liver biopsy as reference standard. This study aimed to investigate the correlation between hepatic steatosis and elastic modulus values measured by SWE and discuss feasibility of SWE for grading steatosis in the absence of fibrosis in NAFLD.

Methods

This study was approved by the animal ethics committee of our university in agreement with committee guidelines.

Animal model construction

All animals were provided by the animal experiment center of our university and fed in the animal room of our university. Eight-week-old male Sprague–Dawley rats ($n=66$) were randomly assigned to two groups after adaptation feeding for a week: A control group ($n=10$) was fed with standard diet, and the experimental group ($n=56$) fed with a methionine choline deficient (MCD) diet. The experimental group underwent US-SWE on the 2nd week ($n=8$), 4th week ($n=8$), 6th week ($n=10$), 8th week ($n=10$), 10th week ($n=10$), and 12th week ($n=10$) to measure various levels of steatosis severity. Similarly, the control group was also studied at 4th week ($n=2$), 6th week ($n=2$), 8th week ($n=2$), 10th week ($n=2$), and 12th week ($n=2$). During the experimental process, rats were had ad libitum access to food and water.

US-SWE examination

Animals' skin was prepared for a better window. All animals were placed on an examination bed in a supine position under anesthesia. The US-SWE device equipped with a Supersonic Imagine Aixplorer with a linear-array transducer and frequency of 4–15 MHz was employed. First, the liver condition, including size, morphology, and echogenicity, was observed in 2D grayscale images, and then the probe was gently fixed on the rats' skin. Subsequently, we switched to SWE mode to display the sampling frame with the appropriate liver parenchyma as examination site, avoiding large vessels, ducts, and inter-lobar fissures [25]. The tissue stiffness in the SWE image ranges from dark blue, indicating the lowest stiffness level (0 kPa), to red, indicating the highest level (up to 70 kPa). Color filling uniformity was > 90% in the sampling frame, considered as successful sampling. After a few seconds, when the SWE image stabilizes, it is frozen and stored. The minimum, mean, maximum elastic

modulus, and standard deviation (SD) in the sampling frame were automatically calculated by the Q-box system using regions of interest (ROI) of 6 mm in diameter approximately (Fig. 1). LSM was performed three times for each subject, and the average of those three acquisitions in kilopascals (kPa) was used for statistical analysis. The above operations were referred to recommendation by EFSUMB Guidelines [21].

Histopathological assessment

After the examination, the rats were sacrificed via intraperitoneal injection of overdose anesthesia, and the liver

was dissected and completely removed. The liver tissue of each animal was stained by hematoxylin and eosin and Masson's trichrome. An experienced pathologist blinded to elastic module values and diet reviewed the biopsy specimens and scored the histologic findings. The scoring system comprised histological features evaluated according to the semi-quantitative NAFLD activity score [26]: Steatosis (0–3), lobular inflammation (0–3), hepatocellular ballooning (0–2), and fibrosis stages (0–4). Steatosis stages were determined by the percentage of hepatocytes containing intracytoplasmic fat droplets. The pathological findings of animals were classified into normal, mild

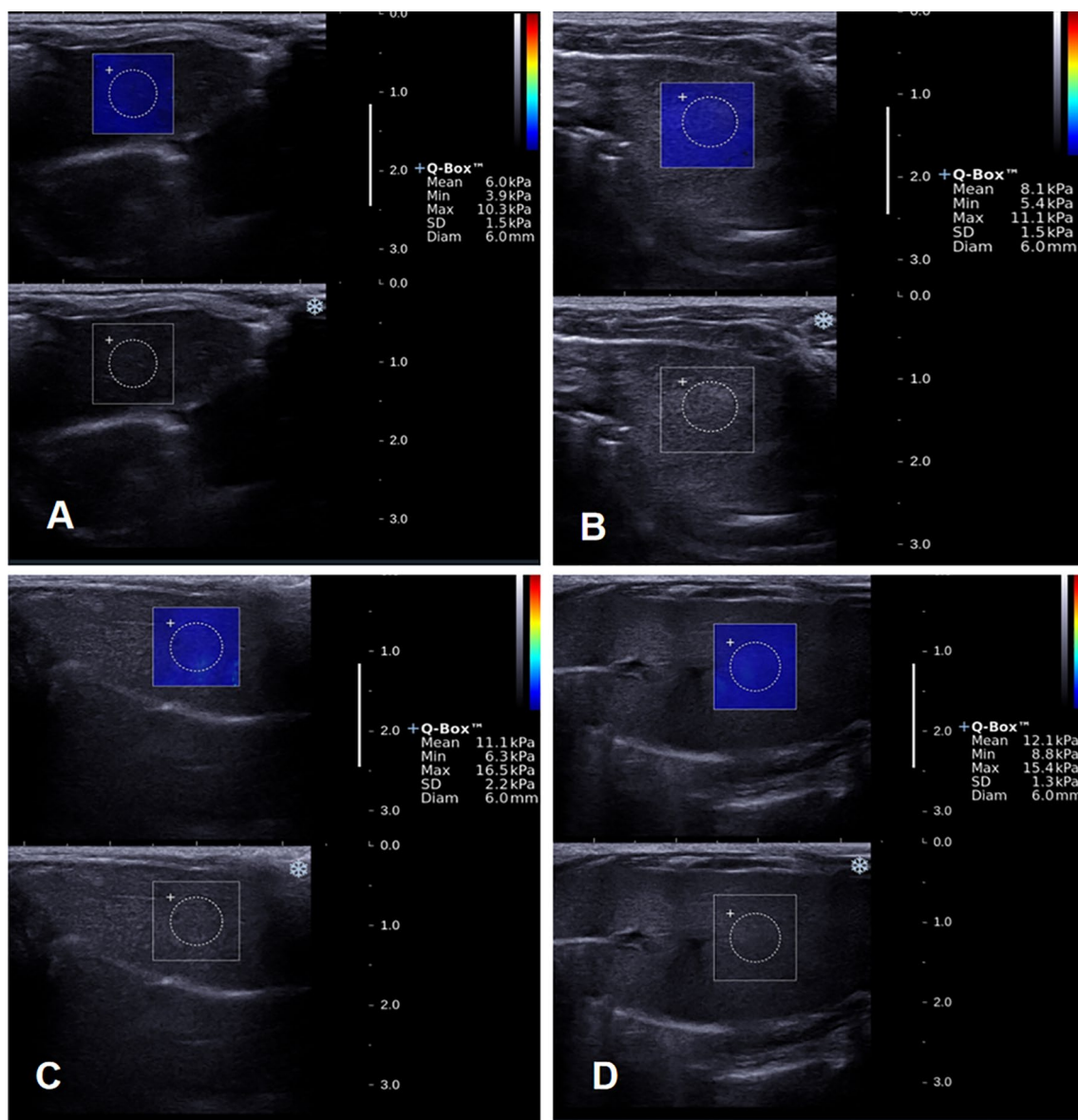


Fig. 1 US-SWE diagrams of steatosis with different degrees in NAFLD. **A** Normal **B** Mild steatosis **C** Moderate steatosis **D** Severe steatosis. Mean, minimum, maximum elastic modulus, and SD values of various degrees are illustrated in the corresponding graphs

steatosis, moderate steatosis, and severe steatosis groups [27]. The staging characteristics of histological findings are shown in Table 1.

Statistical analysis

Continuous variables are expressed as median and interquartile range (IQR). The correlation between histopathologic findings (steatosis, inflammation, and ballooning) and four parameters from US-SWE (mean, maximum, minimum elastic modulus values, and SD) was investigated using Spearman’s rank correlation analysis. Multivariate regression analysis was performed to test the relationship between mean elastic value and pathological features. A post hoc Games–Howell test after one-way analysis of variance was used to compare differences among groups of histopathologic findings. The predictive performance for differentiating steatosis stages was estimated according to the area under ROC curve (AUROC). The optimal threshold was determined by maximizing the Youden index (equal to the sum of sensitivity and specificity minus 1), and also the sensitivity, specificity, positive predictive values (PPVs), and negative predictive values (NPVs) associated with 95% confidence interval (95%CI) were calculated. Decision curve analysis (DCA) was conducted to determine clinical usefulness and the area under decision curve (AUDCA) calculated. Data were analyzed using SPSS, Stata, the statistical software packages R (<http://www.R-project.org>, The R Foundation), and EmpowerStats (<http://www.empowerstats.com>, X&Y Solutions, Inc, Boston, MA). $P < 0.05$ indicates statistical significance.

Results

Animal model and histological findings

A total of 66 rats were used in this study, of which 60 survived and 6 in the MCD group were naturally sacrificed. Specifically, three rats died in the 6th week, 8th week, and 10th week, respectively; the other three rats died in the 12th week, which may be due to intolerance to anesthetics and abdominal effusion. Meanwhile, 10 rats in the control group survived. Given that the presence of fibrosis might be a significant confounding

factor, rats with fibrosis ($n = 12$) were excluded in this study. Ultimately, 48 rats were eligible for the final analysis. All enrolled animals were classified into a normal (14/48, 29.1%), mild steatosis (5/48, 10.4%), moderate steatosis (6/48, 12.5%), and severe steatosis (23/48, 47.9%) groups.

The distribution of pathological features in NAFLD at different time points is summarized in Table 2, and histological sections of NAFLD with various degrees of steatosis are displayed in Fig. 2. Under the microscope, the structure of the lobular liver in the control group was normal, with clear hepatic lamina structure and sinusoids arranged in a spoked shape. Simultaneously, the nucleus was in the cell center, without fat droplets within the cell. The liver of rats in the experimental group showed multiple manifestations of different degrees of steatosis: For mild steatosis: Scattered fat droplets in hepatocytes, present hepatic lamina and sinusoids, and centered nucleus. Moderate steatosis: Many fat droplets in hepatocytes and some compressed and displaced nuclei. Severe steatosis: Liver cells were filled with numerous fat droplets, compressed and displaced nuclei, disorganized liver structure, and lost hepatic blood sinus structure.

Table 2 Distribution of pathological features in NAFLD at different time points

Rearing time	Histological findings			
	Steatosis S0/S1/S2/ S3	Inflammation I0/I1/I2/I3	Ballooning B0/B1/B2	Fibrosis F0/F1/F2/ F3/F4
2w ($n = 8$)	6/2/0/0	0/3/5/0	5/3/0	8/0/0/0/0
4w ($n = 10$)	2/2/2/4	2/4/2/2	9/1/0	10/0/0/0/0
6w ($n = 11$)	2/2/1/6	6/5/0/0	7/1/3	10/0/1/0/0
8w ($n = 11$)	1/0/3/7	2/9/0/0	5/1/5	11/0/0/0/0
10w ($n = 11$)	1/0/1/9	2/8/1/0	10/1/0	7/3/1/0/0
12w ($n = 9$)	2/3/1/3	1/4/0/4	7/1/1	2/3/0/2/2

Data represent the number of pathologic features

Table 1 Stages of histological features with NAFLD

Histological features	Stages				
	0	1	2	3	4
Steatosis	< 5%	5–33%	34–66%	> 66%	–
Lobular inflammation	None	1–2foci/200 × field	2–4foci/200 × field	> 4foci/200 × field	–
Hepatocyte ballooning	None	few balloon cells	Many balloon cells	–	–
Fibrosis	None	Perisinusoidal /periportal	Perisinusoidal and portal/ periportal	Bridging fibrosis	Cirrhosis

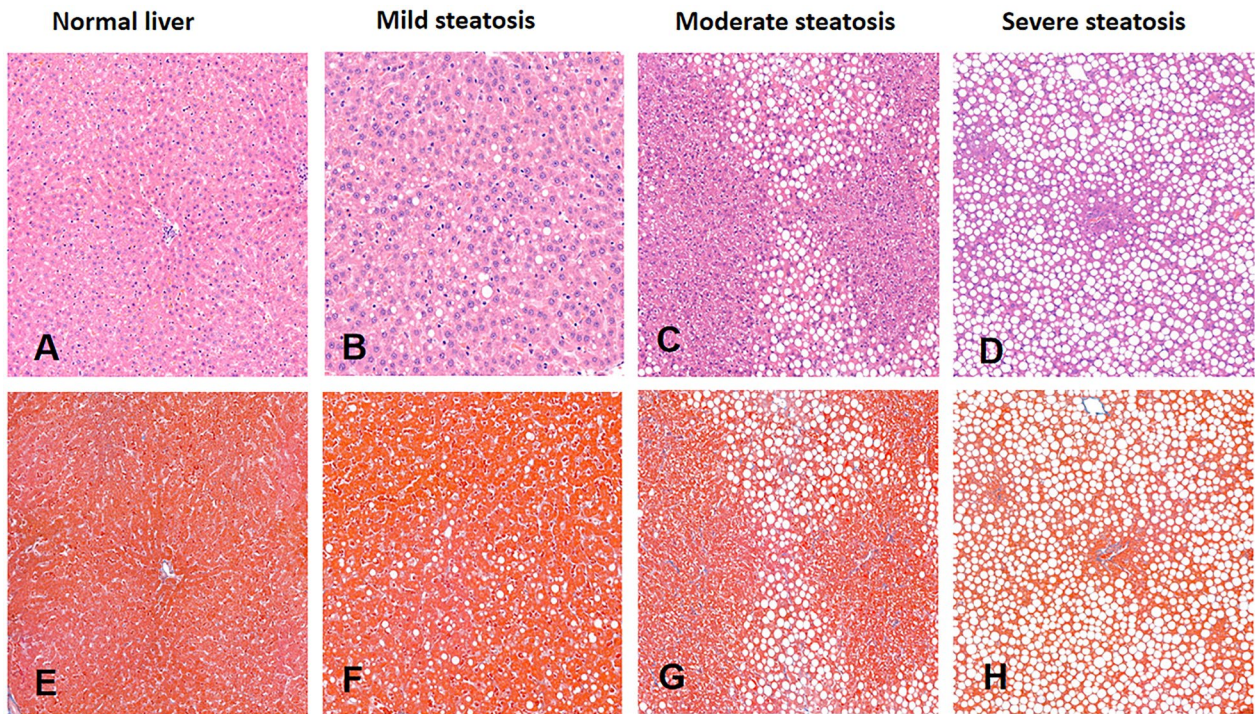


Fig. 2 Histological NAFLD sections with different degrees of steatosis. **A** and **E** Hematoxylin and eosin staining and masson trichrome staining demonstrating the pathological features of steatosis in normal liver, **B** and **F** mild fatty liver, **C** and **G** moderate liver, **D** and **H** severe fatty liver

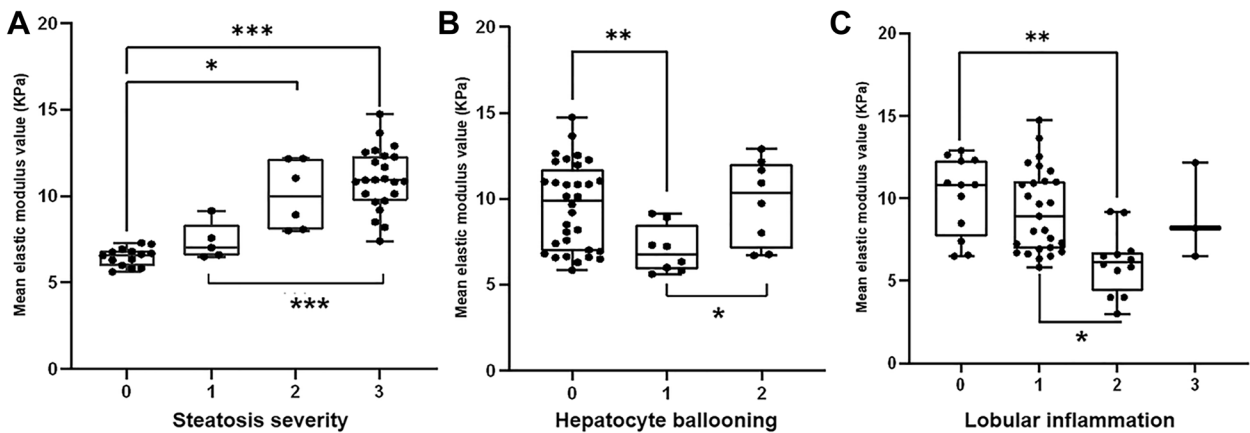


Fig. 3 Distribution of elasticity values in pathological features. The boundaries in box plots show upper and lower quartiles, and the lines in the box the median. Asterisks (*) indicate a Games–Howell test with significant differences

Histopathological features and mean elastic value

The median of the mean elastic modulus values of normal, mild, moderate, and severe groups were 6.60 kPa (IQR: 6.08, 6.79), 7.02 kPa (IQR: 6.60, 7.58), 9.98 kPa (IQR: 8.28, 11.88), and 10.92 kPa (IQR: 9.93, 12.30), respectively. The distribution of mean modulus values according to histological features is illustrated in box plots (Fig. 3). The mean elastic modulus steadily

increased with steatosis stages. As for lobular inflammation, the mean elastic modulus value was highest in grade 0, initially decreased with inflammation degree, reached the lowest value in grade 2, and increased slightly in grade 3. Regarding hepatocellular ballooning, there were significant differences in mean elastic modulus between grades 0 and 2, as well as between grades 1 and 2.

Correlation and multivariate regression analysis

The correlation between elastic modulus values and histological findings is shown in Fig. 4. Steatosis ($\rho=0.81$, $P<0.001$) and lobular inflammation ($\rho=-0.335$, $P=0.03$) were significantly correlated with liver mean elastic value, but hepatocyte ballooning was not significantly correlated with elastic modulus value ($\rho=-0.143$, $P=0.333$). In multivariate analysis, steatosis was an independent factor affecting the mean elastic modulus ($B=1.558$, $P<0.001$), whereas inflammation ($B=-0.031$, $P=0.920$) or ballooning ($B=0.216$, $P=0.458$) was not. Table 3 shows increased elasticity of different degrees of steatosis compared to the normal status. The mean elastic

modules in mild, moderate, and severe steatosis groups were higher [0.88 kPa (95%CI: -0.64 to 2.40, $P=0.261$), 3.57 kPa (95%CI: 2.15-4.99, $P<0.001$), and 4.51 kPa (95%CI: 3.52-5.50, $P<0.001$)] than those in the normal group. After adjusting for inflammation, ballooning, and both, the mean elastic modulus values changed accordingly, but the mean elastic modulus value with moderate or severe steatosis was still higher than that in the normal group ($P<0.001$).

The performance of SWE on evaluation of NAFLD steatosis

The performance of mean elastic modulus in grading the steatosis was analyzed by ROC. Our results showed that the AUROC of the mean elastic modulus model for identifying $\geq S1$ was 0.964 (95%CI: 0.917-1.000), for distinguishing $\geq S2$ it was 0.987 (95%CI: 0.963-1.000), and for differentiating $S=3$ it was 0.904 (95%CI: 0.812-0.996). The corresponding optimal threshold, sensitivity, specificity, PPVs, and NPVs are summarized in Table 4. After adjusting for inflammation and ballooning, the AUROCs for mean elastic modulus for the prediction of steatosis stages were >0.90 regardless of the presence or absence of inflammation and ballooning. The DCA of mean elastic modulus values is presented in Fig. 5. The AUDCA for identifying $\geq S1$ was 0.621, for distinguishing $\geq S2$ it was 0.506, and for differentiating $S=3$ it was 0.256.

Discussion

This study aims to demonstrate the influence of steatosis on liver stiffness measured by SWE on a rat model in the absence of fibrosis, indicating that steatosis, but not inflammation ($B=-0.031$, $P=0.920$) and ballooning ($B=0.216$, $P=0.458$), was an independent factor affecting the mean elastic modulus ($B=1.558$, $P<0.001$). In terms of predictive efficacy, the AUROC of the mean elastic modulus model for differentiating steatosis was >0.90 . After adjusting for inflammation and ballooning, the

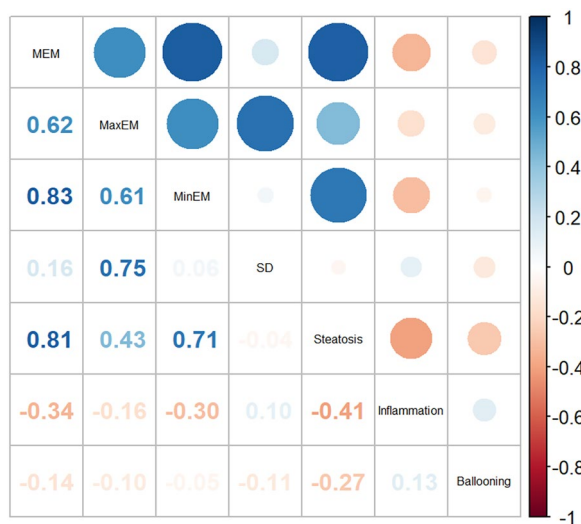


Fig. 4 Correlation between elasticity value and pathological features. The red circle represents a negative correlation, the blue circle a positive correlation; the value in the lower left corner represents the correlation coefficient in Spearman's rank correlation analysis. MEM mean elastic modulus value, MaxEM maximum elastic modulus value, MinEM minimum elastic modulus value, SD standard deviation.

Table 3 Association between NAFLD steatosis stages and mean elastic values adjusted for other pathological features

Parameters	Non-adjusted	Adjust I	Adjust II	Adjust III
S0	Reference	Reference	Reference	Reference
S1	0.88 (-0.64, 2.40) kPa 0.261	0.96 (-0.60, 2.52) kPa 0.235	0.94 (-0.66, 2.54) kPa 0.255	0.97 (-0.67, 2.61) kPa 0.251
S2	3.57 (2.15, 4.99) kPa <0.001	3.42 (1.85, 4.99) kPa <0.001	3.54 (2.04, 5.04) kPa <0.001	3.40 (1.76, 5.05) kPa <0.001
S3	4.51 (3.52, 5.50) kPa <0.001	4.49 (3.35, 5.64) kPa <0.001	4.53 (3.37, 5.69) kPa <0.001	4.50 (3.22, 5.78) kPa <0.001

Data presented by β (95%CI) P value; Independent variable: Steatosis grades; Dependent variable: Mean elastic modulus

Non-adjusted model: None

Adjust I: Model adjusted for inflammation of histological features in rat NAFLD model

Adjust II: Model adjusted for ballooning of histological features in rat NAFLD model

Adjust III: Model adjusted for inflammation and ballooning of histological features in rat

Table 4 The predictive efficiency of SWE for NAFLD assessment

Steatosis	S \geq S1	S \geq S2	S = S3
AUC (95%CI)	0.964 (0.917, 1.000)	0.987 (0.963, 1.000)	0.904 (0.812, 0.996)
AUC* (95%CI)	0.956 (0.872, 0.998)	0.987 (0.951, 1.000)	0.920 (0.816, 0.986)
Cutoff	7.35	7.79	8.13
Sensitivity (%)	91.18 (76.32, 98.14)	96.55 (82.24, 99.91)	95.65 (78.05, 99.89)
Specificity (%)	100.00 (76.84, 98.14)	94.74 (73.97, 99.87)	80.00 (59.30, 93.17)
PPV (%)	100.00 (88.78, 100.00)	96.55 (82.24, 99.91)	81.48 (61.92, 93.70)
NPV (%)	82.35 (56.57, 96.20)	94.74 (73.97, 99.87)	95.24 (76.18, 99.88)
Accuracy (%)	93.75 (82.80, 98.69)	95.83 (85.75, 99.49)	87.50 (74.75, 95.27)

Cutoff critical cutoff value, AUC area under the receiver operating characteristic curve, PPV positive predictive value, NPV negative predictive value

AUC* adjusted for inflammation and ballooning

S \geq S1 fatty liver, S \geq S2 moderate steatosis or higher severity, S = S3 severe steatosis

AUROC of the mean elastic modulus value for distinguishing the steatosis degree was also ≥ 0.92 , which means SWE has excellent predictive validity for grading the steatosis stages regardless of the presence or absence of inflammation and ballooning.

SWE can quantitatively reflect tissue stiffness according to shear wave propagation in the tissue expressed as Young's modulus. Zhaoke Pi et al. [28] showed that the elasticity values μ attained by SWE in vivo had a significant correlation with liver steatosis in NAFLD in a mouse model. Grimal et al. [29] found a steadily increase of median liver stiffness in rats with NASH, measured by SWE, with exacerbation of steatosis grade. Similarly, our results also suggested that steatosis is highly associated with liver mean elastic modulus. This could be explained because the presence of fat droplets within hepatocytes affects the liver structure and may alter the propagation time of vibration waves in the liver, a crucial principle of 2D-SWE.

However, several studies using SWE found no correlation between hepatic steatosis and elasticity [30–32]. Possible factors accounting for this difference could be experimental operators, steatosis type, unadjusted confounding factor, and different diets animal models. In rats fed with MCD, mainly macrovesicular steatosis developed, whereas mainly microvesicular steatosis was observed in the rats fed with a choline deficient diet [33]. Previous study had suggested that microvesicular steatosis was associated significantly with advanced fibrosis, but macrovesicular steatosis was not [34]. Therefore,

different types of steatosis may affect the LSM through SWE due to the presence or absence of fibrosis. Besides, most research investigated the relationship between fibrosis with steatosis and the elastic value by subgroup analysis. A bidirectional relationship between steatosis and fibrosis is found in patients with NAFLD. Specifically, hepatic steatosis can promote fibrosis in the early stages of NAFLD, while advanced fibrosis or cirrhosis reduces the steatosis degree [35]. Consequently, it is difficult to distinguish their separate effects on LSM without adjusting for confounding factors.

In addition, multivariate regression analysis demonstrated that neither inflammation nor ballooning was independently related to liver stiffness, in accordance with previous studies [36, 37]. However, our findings differed from Sugimoto et al.'s [38] and Takeuchi et al.'s [39]. This may be due to differences in experimental subjects, viscoelasticity parameters, and the inherent limitations of non-invasive imaging methods. Interestingly, some studies in NAFLD patients pointed out that inflammation affected LSM accuracy with TE rather than with SWE [17, 31]. Accordingly, inflammation may lead to an increase in LSM with TE but not with 2D-SWE; a combination of TE and 2D-SWE could help identify suitable individuals with inflammation for participation in clinical trials.

Hepatic steatosis and lobular inflammation are strongly associated with NASH progression [40]. To diagnose NASH as early as possible, more attention should be drawn for diagnosis of steatosis. In our study, a rat model was used to limit the confounding effects of fibrosis; our results demonstrated that steatosis was an independent factor affecting elastic modulus, and the AUROC of mean elastic modulus value is >0.90 . Our results indicated that LSM can provide useful information on the status of hepatic steatosis obtained by SWE with or without inflammation and ballooning. Compared to other elastography techniques, SWE can detect tissue elasticity in real time and steadily when observing two-dimensional morphology, allowing to easily select the ideal ROI for measurement of liver elasticity, thus offering more reliable estimates of elastic values.

Some advantages of our study are worth recapitulating. Firstly, at present the "gold standard" for diagnosing NAFLD is liver biopsy. However, it is not suitable for wide application due to its invasiveness, sampling error, and associated complications. Therefore, we established an animal NAFLD model to obtain imaging information and pathological data and accurately assess NAFLD histological features in SWE. Secondly, we demonstrated the influence of steatosis on liver stiffness measured by SWE by adjusting for inflammation and ballooning, and excluding fibrosis. We obtained the estimated effect

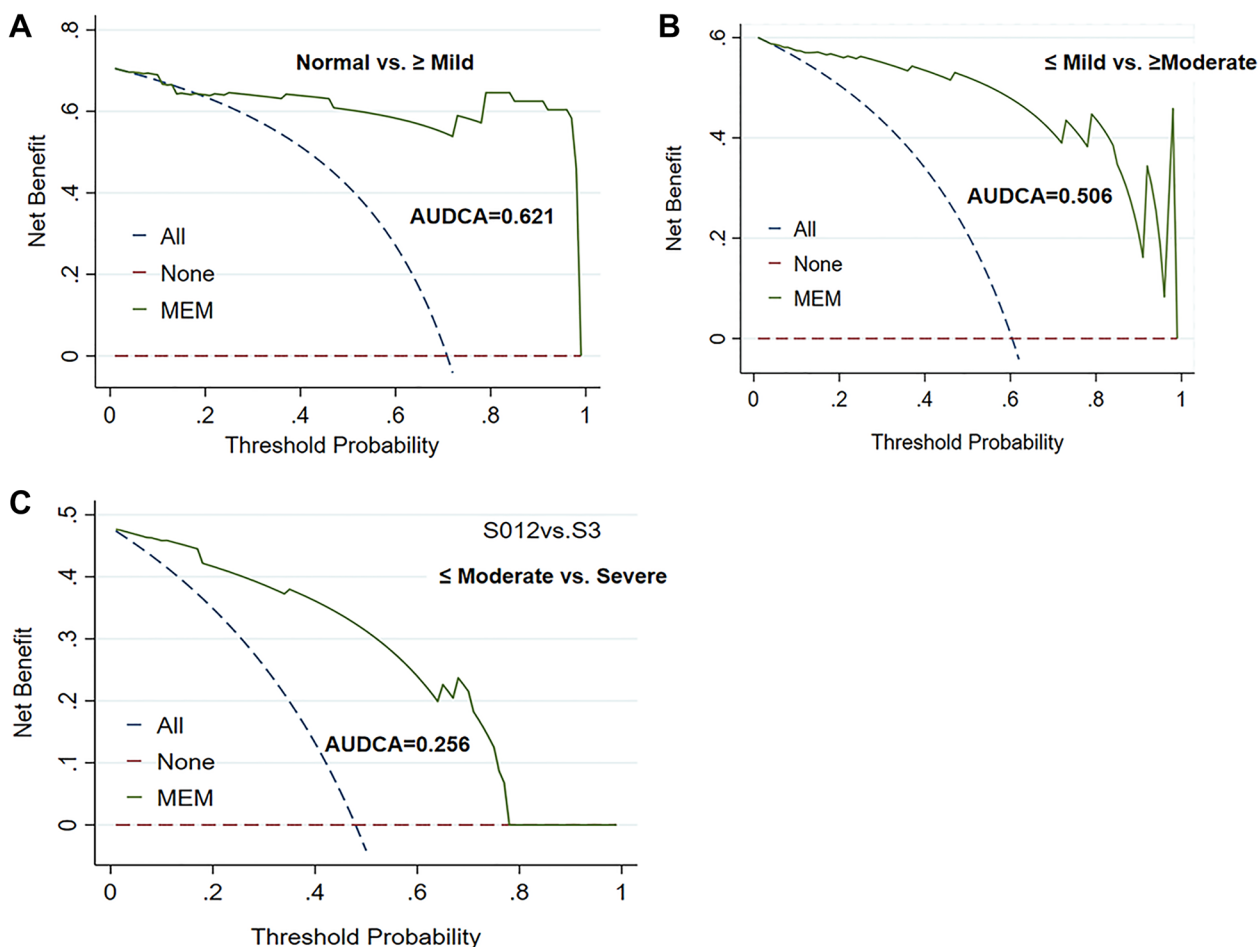


Fig. 5 Decision curve analysis (DCA) of mean elastic modulus value of US-SWE. **A** AUDCA for identifying normal liver and mild steatosis or higher severity was 0.621. **B** AUDCA for distinguishing normal or mild steatosis and moderate or higher severity was 0.506. **C** AUDCA for differentiating severe steatosis and moderate or lower severity was 0.256. MEM mean elastic modulus value, AUDCA area under decision curve analysis

through multiple regression and determined an association between elasticity and steatosis stages. Thirdly, we evaluated the predictive performance of the mean elastic modulus value for steatosis by ROC analysis, as well as the AUC value adjusted by inflammation and ballooning, and DCA and AUDCA were calculated in this study.

Several limitations should be acknowledged. Firstly, an NAFLD animal model could develop a single pathological feature like steatosis, then evaluating its impact on liver stiffness measurement, which would be preferred. With prolonged feeding of MCD, rats develop other pathological features, such as inflammation and fibrosis, that may interfere with the purpose of this study, even though we utilized the statistical approach to adjust. Secondly, to explore the association between steatosis and elastic modules, we excluded rats with fibrosis, as it has been associated with liver stiffness [16], which leads to a relatively small sample size and

may induce sampling error. In addition, the proportion of rats with different degrees of steatosis was uneven, especially in the severe steatosis group. Thirdly, the animal model in our study were Sprague–Dawley rats. Rodents and humans have markedly different metabolic rates, affecting liver homeostasis [30]. Consequently, NAFLD pathogenesis may not exactly replicate in humans; so further research is required to validate and improve SWE accuracy.

In conclusion, mean elasticity was significantly associated with hepatic steatosis rather than ballooning or inflammation. The elasticity measured by SWE can reflect the grades of hepatic steatosis to a certain extent. Despite the usefulness of liver biopsy, SWE may have the feasibility to be introduced as an assistive technology for patients with NAFLD in grading steatosis. Further studies with prospective, more scientific research modalities

and larger sample sizes are needed to clinically validate our results.

Abbreviations

ARFI	Acoustic radiation force impulse
AUDCA	Area under decision curve analysis
AUROC	Area under the receiver operating characteristics curve
CAP	Controlled attenuation parameter
CI	Confidence interval
DCA	Decision curve analysis
HS	Hepatic steatosis
IQR	Interquartile range
LB	Liver biopsy
LISA	Liver ultrasound attenuation
LSM	Liver stiffness measurement
MCD	Methionine choline efficiency
MEM	Mean elastic modulus value
MaxEM	Maximum elastic modulus value
MinEM	Minimum elastic modulus value
NAFLD	Non-alcoholic fatty liver disease
NASH	Non-alcoholic steatohepatitis
NPV	Negative predictive values
PPV	Positive predictive values
SWE	Ultrasound shear wave elastography
SD	Standard deviation
TE	Transient elastography
US	Ultrasound

Acknowledgements

The authors thank all the participants gratefully and staff in the Affiliated Hospital of Guizhou Medical University. They are also thankful to the members of StudyForBetter Team who contributed their best research spirits during the process of the project.

Author contributions

PGL, QHD, and PL contributed to the study concepts. PGL, LWC, and YHW analyzed data and revised the draft; YHW, QJL, YW, PGL, and FY reviewed the literature and drafted the original manuscript. YHW, QJL, PGL, YW, FYL, and YW participated in experiments and data collection. All the authors read and approved the final manuscript.

Funding

This work was supported partly by National Natural Science Foundation of China (Grants no. 81960338), the Science and Technology Projects of Guizhou Province (Qiankehe Support [2020] 4Y193), and Hong Kong Scholar Program.

Availability of data and materials

The datasets are available from the corresponding author with reasonable request.

Declarations

Ethics approval and consent to participate

This study was approved by the institutional review board of our university.

Informed consent

Not applicable.

Consent for publication

Not applicable.

Competing interests

The authors declare that they have no competing interests.

Received: 14 June 2022 Accepted: 3 February 2023

Published online: 11 February 2023

References

- Fouad Y, Waked I, Bollipo S, Gomaa A, Ajlouni Y, Attia D. What's in a name? Renaming "NAFLD" to "MAFLD." *Liver Int.* 2020;40(6):1254–61.
- Fujii H, Kawada N, Japan SGON. The role of insulin resistance and diabetes in nonalcoholic fatty liver disease. *Int J Mol.* 2020;21(11):3863.
- Eslam M, Sanyal AJ, George J. MAFLD: a consensus-driven proposed nomenclature for metabolic associated fatty liver disease. *Gastroenterology.* 2020;158(7):1999–2014.
- Grandison GA, Angulo P. Can nash be diagnosed, graded, and staged noninvasively? *Clin Liver Dis.* 2012;16(3):567–85.
- Pagadala MR, McCullough AJ. The relevance of liver histology to predicting clinically meaningful outcomes in nonalcoholic steatohepatitis. *Clin Liver Dis.* 2012;16(3):487–504.
- Castera L, Friedrich-Rust M, Loomba R. Noninvasive assessment of liver disease in patients with nonalcoholic fatty liver disease. *Gastroenterology.* 2019;156(5):1264–81.
- Lupsor-Platon M, Stefanescu H, Muresan D, Florea M, Szasz ME, Maniu A, et al. Noninvasive assessment of liver steatosis using ultrasound methods. *Med Ultrason.* 2014;16(3):236–45.
- Borges VF, Diniz AL, Cotrim HP, Rocha HL, Andrade NB. Sonographic hepatorenal ratio: a noninvasive method to diagnose nonalcoholic steatosis. *J Clin Ultrasound.* 2013;41(1):18–25.
- van Werven JR, Marsman HA, Nederveen AJ, Smits NJ, Ten KF, van Gulik TM, et al. Assessment of hepatic steatosis in patients undergoing liver resection: comparison of US, CT, T1-weighted dual-echo MR imaging, and point-resolved 1H MR spectroscopy. *Radiology.* 2010;256(1):159–68.
- Shi KQ, Tang JZ, Zhu XL, Ying L, Li DW, Gao J, et al. Controlled attenuation parameter for the detection of steatosis severity in chronic liver disease: a meta-analysis of diagnostic accuracy. *J Gastroenterol Hepatol.* 2014;29(6):1149–58.
- Sasso M, Miette V, Sandrin L, Beaugrand M. The controlled attenuation parameter (CAP): a novel tool for the non-invasive evaluation of steatosis using Fibroscan. *Clin Res Hepatol Gastroenterol.* 2012;36(1):13–20.
- Gatos I, Drazinos P, Yarmenitis S, Theotokas I, Koskinas J, Koullias E, et al. Liver ultrasound attenuation: an ultrasound attenuation index for liver steatosis assessment. *Ultrasound Q.* 2022;38(2):124–32.
- Dioguardi BM, Imbault M, Ronot M, Faccinetto A, Van Beers BE, Rautou PE, et al. Ultrasonic adaptive sound speed estimation for the diagnosis and quantification of hepatic steatosis: a pilot study. *Ultraschall Med.* 2019;40(6):722–33.
- Bohte AE, van Werven JR, Bipat S, Stoker J. The diagnostic accuracy of US, CT, MRI and 1H-MRS for the evaluation of hepatic steatosis compared with liver biopsy: a meta-analysis. *Eur Radiol.* 2011;21(1):87–97.
- Wong VW, Chu WC, Wong GL, Chan RS, Chim AM, Ong A, et al. Prevalence of non-alcoholic fatty liver disease and advanced fibrosis in Hong Kong Chinese: a population study using proton-magnetic resonance spectroscopy and transient elastography. *Gut.* 2012;61(3):409–15.
- Ferraioli G, Wong VW, Castera L, Berzigotti A, Sporea I, Dietrich CF, et al. Liver ultrasound elastography: an update to the world federation for ultrasound in medicine and biology guidelines and recommendations. *Ultrasound Med Biol.* 2018;44(12):2419–40.
- Petta S, Maida M, Macaluso FS, Di Marco V, Camma C, Cabibi D, et al. The severity of steatosis influences liver stiffness measurement in patients with nonalcoholic fatty liver disease. *Hepatology.* 2015;62(4):1101–10.
- Gaia S, Carenzi S, Barilli AL, Bugianesi E, Smedile A, Brunello F, et al. Reliability of transient elastography for the detection of fibrosis in non-alcoholic fatty liver disease and chronic viral hepatitis. *J Hepatol.* 2011;54(1):64–71.
- EASL-ALEH Clinical Practice Guidelines. Non-invasive tests for evaluation of liver disease severity and prognosis. *J Hepatol.* 2015;63(1):237–64.
- Herrmann E, de Ledinghen V, Cassinotto C, Chu WC, Leung VY, Ferraioli G, et al. Assessment of biopsy-proven liver fibrosis by two-dimensional shear wave elastography: an individual patient data-based meta-analysis. *Hepatology.* 2018;67(1):260–72.
- Dietrich CF, Bamber J, Berzigotti A, Bota S, Cantisani V, Castera L, et al. EFSUMB guidelines and recommendations on the clinical use of liver ultrasound elastography, update 2017 (long version). *Ultraschall Med.* 2017;38(4):e16–47.
- Yang J, Lin L, Xue E, Hong D, Yang Y, Xu M, et al. Can nonfibrotic non-alcoholic steatohepatitis be effectively identified by supersonic shear imaging? *Anal Cell Pathol (Amst).* 2019;2019:2013674.

23. Garcovich M, Veraldi S, Di Stasio E, Zocco MA, Monti L, Toma P, et al. Liver stiffness in pediatric patients with fatty liver disease: diagnostic accuracy and reproducibility of shear-wave elastography. *Radiology*. 2017;283(3):820–7.
24. Huang Z, Zhou J, Lu X, Zhang T, Xu S, Jin J, et al. How does liver steatosis affect diagnostic performance of 2D-SWE.SSI: assessment from aspects of steatosis degree and pathological types. *Eur radiol*. 2021;31(5):3207–15.
25. Martins PN, Neuhaus P. Surgical anatomy of the liver, hepatic vasculature and bile ducts in the rat. *Liver Int*. 2007;27(3):384–92.
26. Kleiner DE, Brunt EM, Van Natta M, Behling C, Contos MJ, Cummings OW, et al. Design and validation of a histological scoring system for nonalcoholic fatty liver disease. *Hepatology*. 2005;41(6):1313–21.
27. Lau JK, Zhang X, Yu J. Animal models of non-alcoholic fatty liver disease: current perspectives and recent advances. *J Pathol*. 2017;241(1):36–44.
28. Pi Z, Wang M, Lin H, Guo Y, Chen S, Diao X, et al. Viscoelasticity measured by shear wave elastography in a rat model of nonalcoholic fatty liver disease: comparison with dynamic mechanical analysis. *Biomed Eng Online*. 2021. <https://doi.org/10.1186/s12938-021-00879-3>.
29. Ogawa S, Moriyasu F, Yoshida K, Oshiro H, Kojima M, Sano T, et al. Relationship between liver tissue stiffness and histopathological findings analyzed by shear wave elastography and compression testing in rats with non-alcoholic steatohepatitis. *J Med Ultrason* (2001). 2016;43(3):355–60.
30. Nightingale KR, Rouze NC, Rosenzweig SJ, Wang MH, Abdelmalek MF, Guy CD, et al. Derivation and analysis of viscoelastic properties in human liver: impact of frequency on fibrosis and steatosis staging. *IEEE Trans Ultrason Ferroelectr Freq Control*. 2015;62(1):165–75.
31. Mendoza YP, Rodrigues SG, Delgado MG, Murgia G, Lange NF, Schropp J, et al. Inflammatory activity affects the accuracy of liver stiffness measurement by transient elastography but not by two-dimensional shear wave elastography in non-alcoholic fatty liver disease. *Liver Int*. 2021;42(1):102–11.
32. Cassinotto C, Boursier J, de Ledinghen V, Lebigot J, Lapuyade B, Cales P, et al. Liver stiffness in nonalcoholic fatty liver disease: a comparison of supersonic shear imaging, FibroScan, and ARFI with liver biopsy. *Hepatology*. 2016;63(6):1817–27.
33. Veteläinen R, van Vliet A, van Gulik TM. Essential pathogenic and metabolic differences in steatosis induced by choline or methionine-choline deficient diets in a rat model. *J Gastroenterol Hepatol*. 2007;22(9):1526–33.
34. Tandra S, Yeh MM, Brunt EM, Vuppalanchi R, Cummings OW, Unalp-Arida A, et al. Presence and significance of microvesicular steatosis in nonalcoholic fatty liver disease. *J Hepatol*. 2011;55(3):654–9.
35. Ong JP, Younossi ZM. Epidemiology and natural history of NAFLD and NASH. *Clin Liver Dis*. 2007;11(1):1–16.
36. Lee MS, Bae JM, Joo SK, Woo H, Lee DH, Jung YJ, et al. Prospective comparison among transient elastography, supersonic shear imaging, and ARFI imaging for predicting fibrosis in nonalcoholic fatty liver disease. *PLoS ONE*. 2017;12(11): e188321.
37. Kang BK, Lee SS, Cheong H, Hong SM, Jang K, Lee MG. Shear wave elastography for assessment of steatohepatitis and hepatic fibrosis in rat models of non-alcoholic fatty liver disease. *Ultrasound Med Biol*. 2015;41(12):3205–15.
38. Sugimoto K, Moriyasu F, Oshiro H, Takeuchi H, Yoshimasu Y, Kasai Y, et al. Viscoelasticity measurement in rat livers using shear-wave US elastography. *Ultrasound Med Biol*. 2018;44(9):2018–24.
39. Takeuchi H, Sugimoto K, Oshiro H, Iwatsuka K, Kono S, Yoshimasu Y, et al. Liver fibrosis: noninvasive assessment using supersonic shear imaging and FIB4 index in patients with non-alcoholic fatty liver disease. *J Med Ultrason* (2001). 2018;45(2):243–9.
40. Yoshioka Y, Hashimoto E, Yatsuji S, Kaneda H, Taniai M, Tokushige K, et al. Nonalcoholic steatohepatitis: cirrhosis, hepatocellular carcinoma, and burnt-out Nash. *J Gastroenterol*. 2004;39(12):1215–8.

Publisher's Note

Springer Nature remains neutral with regard to jurisdictional claims in published maps and institutional affiliations.

Ready to submit your research? Choose BMC and benefit from:

- fast, convenient online submission
- thorough peer review by experienced researchers in your field
- rapid publication on acceptance
- support for research data, including large and complex data types
- gold Open Access which fosters wider collaboration and increased citations
- maximum visibility for your research: over 100M website views per year

At BMC, research is always in progress.

Learn more biomedcentral.com/submissions

